JACS
JOURNAL OF THE AMERICAN CHEMICAL SOCIETY

Article

pubs.acs.org/JACS

Two-Photon Neuronal and Astrocytic Stimulation with Azobenzene-Based Photoswitches

Mercè Izquierdo-Serra,[†,+] Marta Gascón-Moya,[‡,+] Jan J. Hirtz,[§] Silvia Pittolo,[†] Kira E. Poskanzer,[§] Èric Ferrer,[†,‡] Ramon Alibés,[‡] Félix Busqué,[‡] Rafael Yuste,*[,§] Jordi Hernando,*[,‡] and Pau Gorostiza*[,†,∥,⊥]

[†]Institut de Bioenginyeria de Catalunya, 08028 Barcelona, Spain

[‡]Departament de Química, Universitat Autònoma de Barcelona, 08193 Cerdanyola del Vallès, Spain

[§]Department of Biological Sciences, Columbia University, New York, New York 10027, United States

[∥]Centro de Investigación Biomédica en Red en Bioingeniería, Biomateriales y Nanomedicina, 50018 Zaragoza, Spain

[⊥]Institució Catalana de Recerca i Estudis Avançats, 08010 Barcelona, Spain

Supporting Information

ABSTRACT: Synthetic photochromic compounds can be designed to control a variety of proteins and their biochemical functions in living cells, but the high spatiotemporal precision and tissue penetration of two-photon stimulation have never been investigated in these molecules. Here we demonstrate two-photon excitation of azobenzene-based protein switches and versatile strategies to enhance their photochemical responses. This enables new applications to control the activation of neurons and astrocytes with cellular and subcellular resolution.

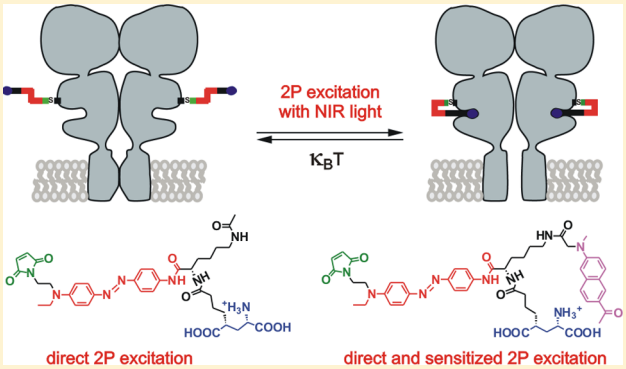

INTRODUCTION

The large number of photoswitchable biomolecules discovered and developed in recent years covers a great variety of cellular functions, like catalysis of metabolic processes,[1,2] cytoskeletal polymerization[3] and motors,[2,4] nucleic acids dynamics,[5−7] intracellular signaling,[8,9] and, perhaps most dazzling, membrane excitability, which has been at the focus of optogenetics[10] and optopharmacology.[11] The dream of precisely and remotely photocontrolling every aspect of the cell's inner workings in intact tissue appears within reach and offers the promise of interrogating complex cellular processes to discover their molecular mechanisms.[12]

In order to take full advantage of light-regulated proteins, multiphoton excitation with near-infrared (NIR) light provides sub-micrometric resolution in three dimensions,[13] deep penetration into tissue,[14] and patterned illumination.[15,16] However, to be adapted to two-photon stimulation technology, the light response of natural photoswitchable proteins like Channelrhodopsin-2 (ChR2) must often be adjusted by mutating the tight binding pocket of the natural chromophore, which has fixed photochemical characteristics.[17,18] In contrast, synthetic photoswitches developed by optochemical genetics and optopharmacology are based on chromophores that act on the protein surface and thus offer excellent opportunities for rationally tuning their photochemical behavior by chemical substitutions that do not affect the functional properties of the protein.[19−22] Remarkably, two-photon stimulation of synthetic photoswitchable proteins has not been investigated despite the advances of neurotransmitter uncaging[23] and optogenetics[24,25] using pulsed NIR illumination.

To demonstrate the multiphoton activation of synthetic photoswitches, we chose ion channels because they constitute highly sensitive transducers of chromophore isomerization (potentially up to the single channel level). In particular, we focused on the well-characterized light-gated glutamate receptor (LiGluR),[26,27] a GluK2 kainate receptor-channel that is chemically conjugated to a maleimide−azobenzene−glutamate photoswitch (MAG **1**, Figure 1a). Azobenzene *trans*−*cis* photoisomerization[28] of this photoswitchable tethered ligand (PTL) allows the efficient activation of the receptor upon one-photon absorption of violet or blue radiation (open LiGluR, Figure 1b), a process that can be reverted back either by absorption of green light or thermal relaxation in the dark (closed LiGluR, Figure 1b).[21,26,27]

To control LiGluR using multiphoton excitation, here we have investigated the performance of MAG and two new MAG derivatives (**2** and **3**, Figure 1a) upon pulsed NIR illumination. Compounds **2** and **3** were devised to enhance the two-photon excitation response of the symmetrically substituted azoben-

Received: March 19, 2014
Published: May 23, 2014

   dx.doi.org/10.1021/ja5026326 | J. Am. Chem. Soc. 2014, 136, 8693−8701

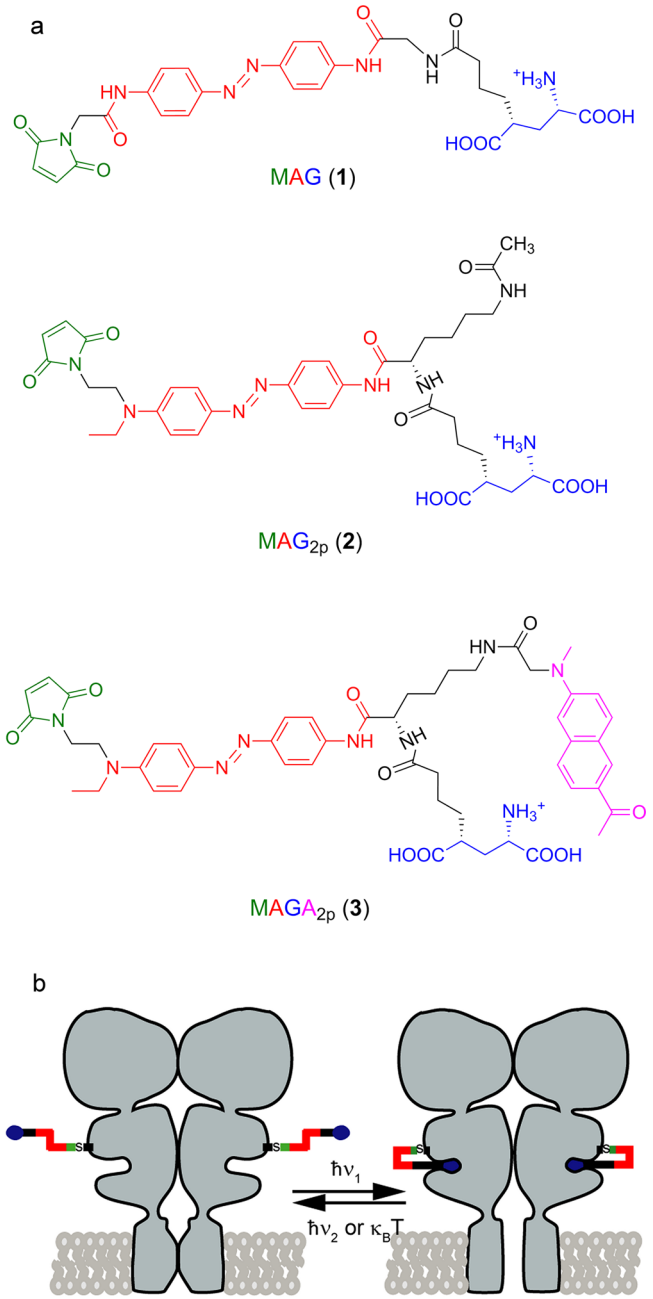

Figure 1. (a) Structures of the photoswitchable tethered ligands applied to the two-photon control of LiGluR: MAG (**1**), MAG_{2p} (**2**), and $MAGA_{2p}$ (**3**). (b) Operating mode of different PTLs on LiGluR. Violet (one-photon) or NIR (two-photon) light excitation induces glutamate recognition and channel opening via *trans*–*cis* isomerization, which results in ion flow across the membrane. This process is reverted by illumination with visible light (one-photon excitation) for LiGluR-MAG and by thermal back-isomerization for LiGluR-MAG_{2p} and LiGluR-$MAGA_{2p}$.

zene chromophore in MAG, which is expected to be poor.[29,30] We tested two design concepts using a modular architecture. In compound **2** we introduced an asymmetric aminoazobenzene with sufficiently strong push–pull character as to enhance its two-photon absorption cross-section (MAG_{2p}).[29−32] In addition, the presence of the electron-donating tertiary amine in the 4-position should dramatically decrease the thermal stability of its *cis* state in physiological conditions,[21] thus resulting in fast spontaneous *cis*–*trans* back-isomerization and, as such, enabling single-wavelength operation of the switch. This behavior is also expected for **3** containing the same azobenzene core as MAG_{2p}. However, a novel scheme was exploited in this compound to enhance its nonlinear optical response, which consists in the introduction of a light-harvesting antenna to sensitize the *trans*–*cis* isomerization of the system by absorption of NIR radiation and subsequent resonant electronic energy transfer (RET) to the *trans*-azobenzene group.[33] Because of its maleimide–azobenzene–glutamate–antenna structure, we named compound **3** as $MAGA_{2p}$. A naphthalene derivative was selected as antenna because of (i) its high two-photon absorption cross-section,[34] (ii) the large spectral overlap between its emission and the absorption of the *trans* isomer of the aminoazobenzene group in **3**, and (iii) its reduced size, to minimize potential steric hindrance effects on the glutamate-binding site of the receptor.

RESULTS AND DISCUSSION

Synthesis of MAG_{2p} and $MAGA_{2p}$. The preparation of compounds MAG_{2p} and $MAGA_{2p}$ was achieved via a multistep modular synthetic sequence allowing structural diversity in the final compounds as well as the additional incorporation of a photo-harvesting antenna in **3** (Scheme 1). In both cases, we took the *N*,*N*-orthogonally diprotected L-lysine **4** as scaffold, to which the different functional fragments of the target compounds were sequentially introduced: *O*-protected aminoazobenzene **5**, fully protected glutamate derivative **6**, naphthalene derivative **7**, and furan-protected maleimide **8**. These fragments were obtained from commercial products as described in the Supporting Information. With respect to the synthesis of MAG,[26] several changes were realized in our procedure. First, a branching point was inserted between the glutamate and azobenzene moieties to facilitate the incorporation of additional functional units to the PTL structure. Second, we introduce herein the use of **6** and **8** as more robust, versatile, and convenient precursors of glutamate and maleimide moieties during the multistep synthesis of novel MAG derivatives.

The synthesis of both MAG_{2p} and $MAGA_{2p}$ began by the coupling reaction of **4** with aminoazobenzene **5** to afford the common intermediate **9**, from which the synthetic pathways diverged. For the synthesis of MAG_{2p}, acid removal of the *tert*-butyl carbamate protection of **9** was followed by the coupling reaction of the resulting amine with glutamate derivative **6**, basic deprotection of the terminal amine, and its acetylation to furnish intermediate **12a**. In the case of $MAGA_{2p}$, the best results were obtained by deprotecting first the amino terminus and proceeding through its reaction with the antenna fragment **7** to deliver **11**. Removal of the carbamate protection and coupling with **6** then furnished compound **12b**. From intermediates **12a** and **12b**, the next synthetic steps were analogous for both ligands: removal of the allyl protecting group, introduction of the furan-protected maleimide **8** under Mitsunobu conditions, release of the maleimide moiety via a retro-Diels–Alder reaction, and cleavage of the *tert*-butyl carbamate and ester protections, thus finally affording the target compounds MAG_{2p} and $MAGA_{2p}$.

Photochemical Characterization of MAG_{2p} and $MAGA_{2p}$. Figure 2a plots the electronic absorption spectra of the initial *trans* state of compounds **1**–**3** and of the photo-harvesting antenna tethered to $MAGA_{2p}$ (see also Figures S1 and S2 in the Supporting Information). Owing to the 4-amino substituent introduced in the azobenzene core of *trans*-MAG_{2p}

dx.doi.org/10.1021/ja5026326 | J. Am. Chem. Soc. 2014, 136, 8693−8701

Scheme 1. Total Synthesis of MAG_{2p} (2) and $MAGA_{2P}$ (3)[a]

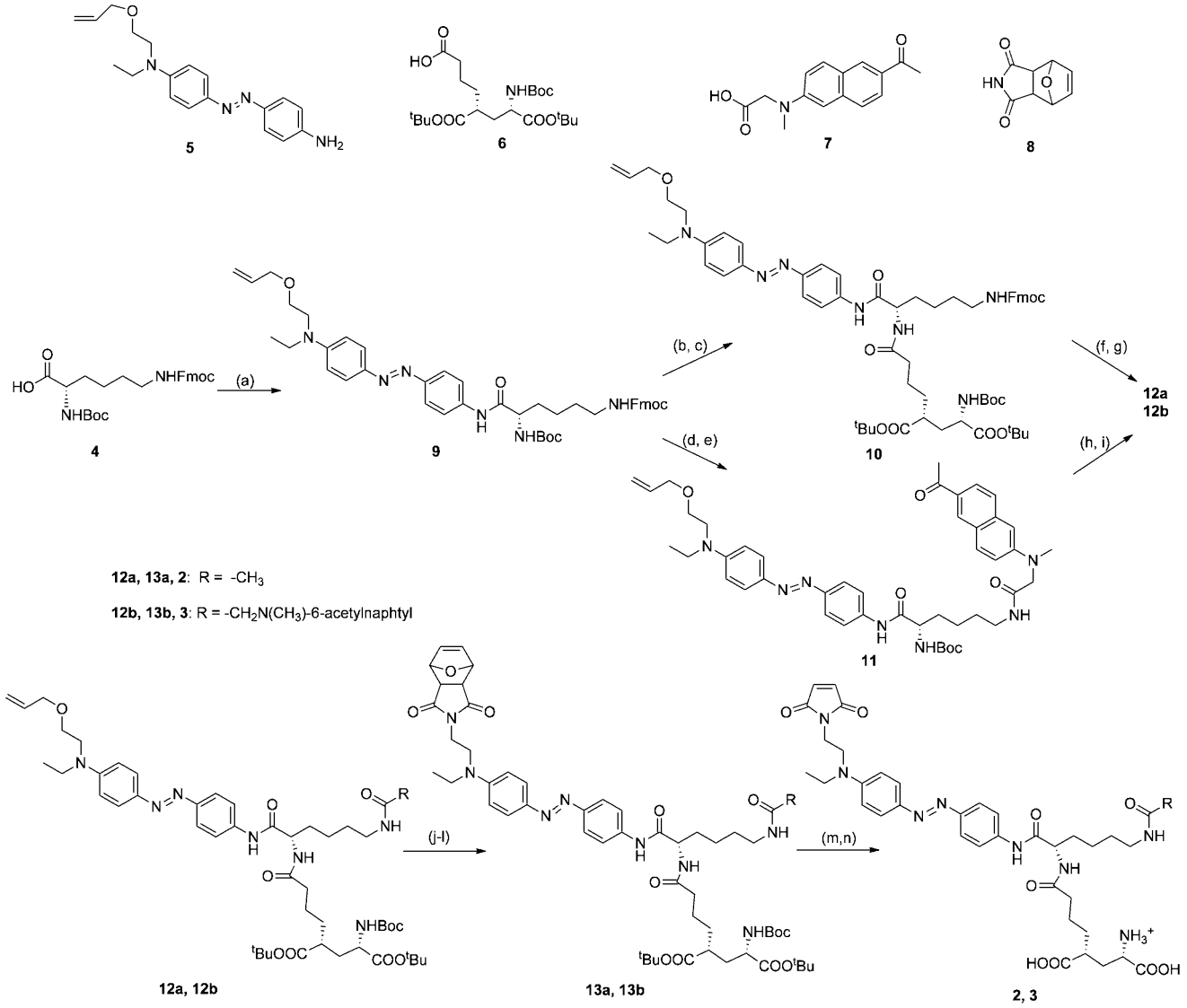

[a]Reagents and conditions: (a) **5**, HATU, DIPEA, THF (89%); (b) 37% HCl, MeOH (93%); (c) **6**, EDCI, HOBt, DIPEA, THF (88%); (d) 20% piperidine/DMF (87%); (e) **7**, EDCI, DIPEA, THF (81%); (f) 20% piperidine/DMF (64%); (g) $ClCOCH_3$, pyridine, THF (69%); (h) 37% HCl, MeOH (93%); (i) **6**, EDCI, HOBt, DIPEA, THF (71%); (j) $RhCl(PPH_3)_3$, $EtOH/H_2O$, reflux; (k) HgO, $HgCl_2$, acetone/H_2O, reflux; (l) **8**, Ph_3P, DIAD, THF (81%, over the three steps, for **13a**, 27% for **13b**); (m) toluene, reflux; (n) TFA, CH_2Cl_2 (81% over the two steps for **2**, 86% for **3**). Abbreviations: HATU, *O*-(7-azabenzotriazol-1-yl)-*N*,*N*,*N*′,*N*′-tetramethyluronium hexafluorophosphate; DIPEA, diisopropylethylamine; EDCI, *N*-ethyl-*N*′-(3-dimethyldiaminopropyl)-carbodiimide HCl; HOBt, 1-hydroxybenzotriazole hydrate; DIAD, diisopropyl azodicarboxylate.

and *trans*-$MAGA_{2p}$,[21,35] the absorption maximum of the azoaromatic $\pi\rightarrow\pi^*$ electronic transition of these compounds clearly bathochromically shifts with respect to *trans*-MAG (∼50 nm in DMSO). This allows the *trans*−*cis* photoisomerization of MAG_{2p} and $MAGA_{2p}$ to occur upon illumination with blue light instead of violet radiation. As shown in Figure 2b, excitation of both ligands at 473 nm led to a noticeable decrease of their $\pi\rightarrow\pi^*$ absorption band, a typical signature of photoinduced *cis* isomer formation.[35] This was further confirmed by ^1H NMR measurements in DMSO-d_6, which revealed that the relative concentration of *cis*-MAG_{2p} and *cis*-$MAGA_{2p}$ in the resulting photostationary mixtures was 58% in both cases. Such photoproducts can be transformed into their corresponding *trans* isomers by irradiation with green light, as previously reported for MAG[26,27] (Figure S3 in the Supporting Information). In the case of MAG_{2p} and $MAGA_{2p}$, however, spontaneous thermal *cis*−*trans* isomerization plays a significant role in the recovery of the initial state of the ligands, and it strongly competes with *cis*−*trans* photoisomerisation due to the lower stability of their *cis* isomers. This effect is ascribed to the introduction of a 4-amino substituent in the azobenzene moiety of MAG_{2p} and $MAGA_{2p}$,[21,35] and it is expected to be dramatically enhanced in aqueous media.[36] Thus, while the lifetimes of *cis*-MAG_{2p} and *cis*-$MAGA_{2p}$ in the dark at room temperature are ∼75 min in DMSO (see Figure S4 in the Supporting Information), they further drop off down to the millisecond time scale in aqueous buffer (τ = 118 and 96 ms in 80% PBS: 20% DMSO, respectively; Figure 2c). This allows repetitive *trans*−*cis* isomerization of MAG_{2p} and $MAGA_{2p}$ at high frequencies in aqueous media with a single irradiation source, which we have exploited to demonstrate the high

dx.doi.org/10.1021/ja5026326 | J. Am. Chem. Soc. 2014, 136, 8693−8701

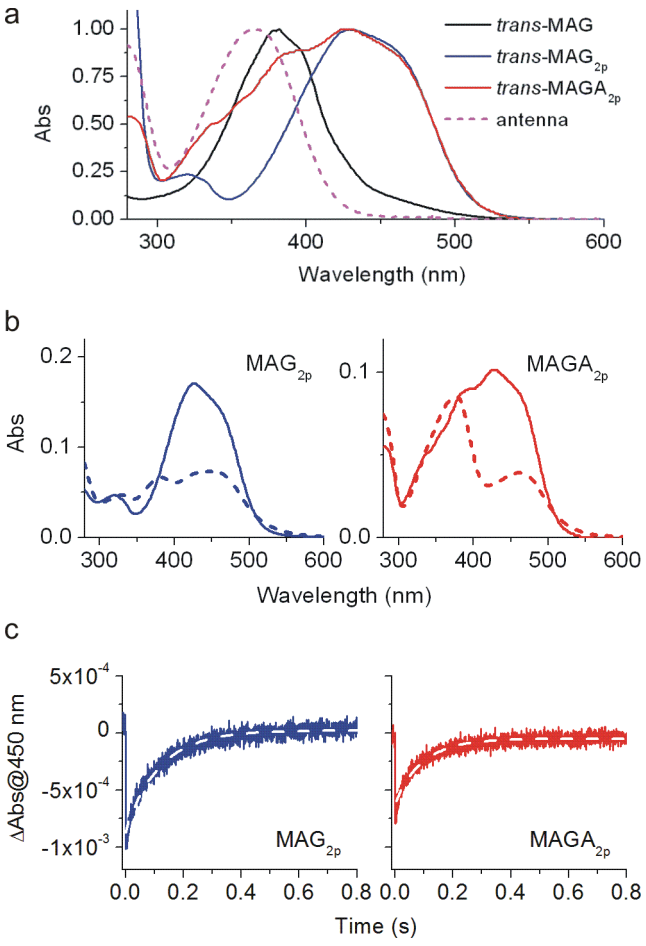

Figure 2. (a) Absorption spectra in DMSO of *trans*-MAG, *trans*-MAG_{2p}, *trans*-$MAGA_{2p}$, and the free naphthalene photo-harvesting antenna. Each spectrum was normalized to its maximum. (b) Absorption spectra of *trans*-MAG_{2p} and *trans*-$MAGA_{2p}$ (solid lines), and the photostationary states obtained upon photoexcitation of these compounds in DMSO at λ_{exc} = 473 nm (dashed lines). (c) Variation of the absorption at λ = 450 nm of *trans*–*cis* mixtures of MAG_{2p} and $MAGA_{2p}$ in the dark at 25 °C in 80% PBS:20% DMSO. At these conditions, thermal *cis*–*trans* back-isomerization takes place, thus restoring the initial concentration of the *trans* state of the ligands, which presents a larger extinction coefficient at λ_{abs} = 450 nm. Solid lines correspond to the experimental data, while dashed lines were obtained from monoexponential fits.

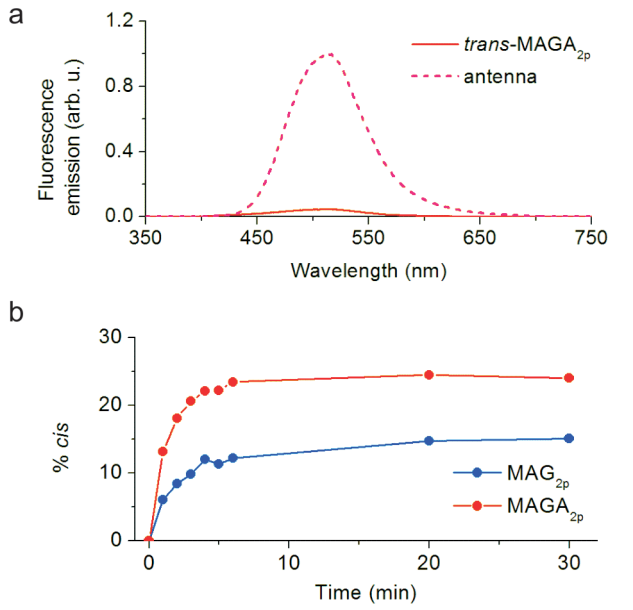

Figure 3. (a) Fluorescence emission spectra in 80% PBS:20% DMSO of *trans*-$MAGA_{2p}$ and the photo-harvesting antenna tethered to this ligand. The spectra are normalized relative to the excitation intensity and the absorption at the excitation wavelength (λ_{exc} = 355 nm). (b) *trans*–*cis* photoconversion efficiency of *trans*-MAG_{2p} and *trans*-$MAGA_{2p}$ upon irradiation at λ = 355 nm in DMSO, which allows nearly selective excitation of *trans*-$MAGA_{2p}$ sensitizer (see Figure 2a).

photostability of these light-responsive ligands (Figure S5 in the Supporting Information).

Although the incorporation of a photo-harvesting antenna negligibly affects the intrinsic photochemical behavior of the azobenzene group of $MAGA_{2p}$ with respect to MAG_{2p}, it provides ligand **3** with some additional optical properties. Thus, *trans*-$MAGA_{2p}$ displays an extra band in the absorption spectrum (λ_{max} = 385 and 380 nm in DMSO and 80% PBS: 20% DMSO, respectively), which arises from the naphthalene sensitizer (Figure 2a and Figure S1 in the Supporting Information). The fluorescence emission of this group is however strongly quenched upon covalent attachment to the ligand, with a ~20-fold decrease in fluorescence quantum yield measured in aqueous buffer ($\Phi_{antenna}$ = 0.43 and $\Phi_{trans\text{-}MAGA2p}$ = 0.02; Figure 3a). This indicates the occurrence of efficient RET processes from the photoexcited naphthalene antenna to the azo moiety of *trans*-$MAGA_{2p}$, in agreement with the large Förster radius calculated for this donor–acceptor pair (see Figure S6 in the Supporting Information). Consequently, photosensitized *trans*–*cis* isomerization should take place in this ligand, as demonstrated in Figure 3b: ~60% increase in *trans*–*cis* photoconversion was determined for $MAGA_{2p}$ with respect to MAG_{2p} upon selective irradiation of the naphthalene antenna at λ_{exc}= 355 nm.

Electrophysiological Characterization of MAG, MAG_{2p}, and $MAGA_{2p}$ under One- and Two-Photon Stimulation. We next tested MAG, MAG_{2p}, and $MAGA_{2p}$ to photoswitch LiGluR in living cells using one- and two-photon stimulation. We expressed GluK2-L439C-eGFP in HEK293 cells and incubated them in MAG, MAG_{2p}, or $MAGA_{2p}$ in order to allow the selective conjugation of the PTLs to the cysteine introduced at position L439C of the receptor. For each compound, we recorded the corresponding photocurrents generated upon light-induced opening of LiGluR channels using whole-cell patch clamp[26,27] (see the Supporting Information).

One-photon LiGluR currents were obtained when the receptor was conjugated with the new compounds (Figures 4 and 5a). The magnitude of the photocurrent response was not reduced after repeated stimulations, demonstrating the photostability of these compounds after protein conjugation (Figure 4b,c and Figure S8 in the Supporting Information). Figure 4 shows that for one-photon excitation, the wavelength dependence of current amplitude measured is different for each PTL. Photocurrent amplitudes at different wavelengths were quantified from electrophysiological recordings obtained for the three compounds (Figure 4a–c), and the corresponding one-photon action spectra were calculated (Figure 4d). Introduction of the 4-amino substituent in the azo core allows the one-photon action spectra of MAG_{2p} and $MAGA_{2p}$ to red-shift ~60 nm with respect to that of MAG, as recently reported

dx.doi.org/10.1021/ja5026326 | J. Am. Chem. Soc. 2014, 136, 8693–8701

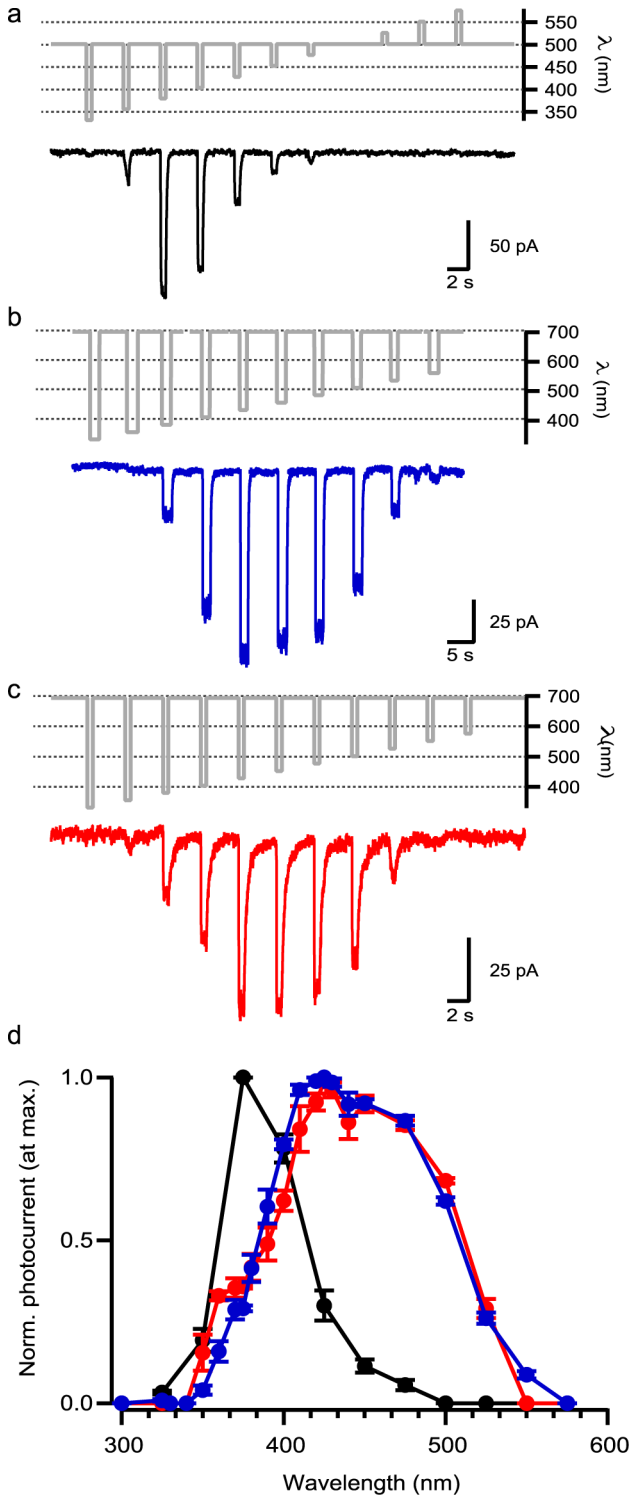

Figure 4. Whole-cell voltage-clamp current recordings in HEK293 cells expressing GluK2-L439C after conjugation to (a) MAG, (b) MAG_{2p}, and (c) $MAGA_{2p}$. Current responses to one-photon light pulses of wavelengths ranging from 325 to 575 nm were quantified. (Note that in (a) resting λ = 500 nm induces LiGluR deactivation, and in (b) and (c) resting λ = 690 nm is not absorbed and allows thermal relaxation of these photoswitches.) (d) Normalized one-photon action spectra corresponding to MAG (black), MAG_{2p} (blue), and $MAGA_{2p}$ (red) (N = 2 cells, N = 3–8 cells, and N = 4–10 cells, respectively). Before averaging over different cells, wavelength-dependent current amplitudes were normalized to the maximum photocurrent along the spectral range measured for each cell. Errors are SEM.

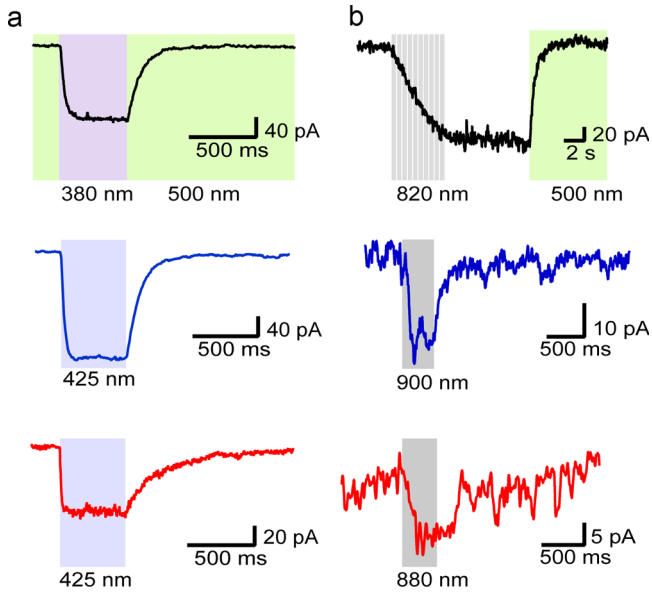

Figure 5. (a) One- and (b) two-photon whole-cell voltage-clamp recordings on HEK293 cells expressing LiGluR conjugated with MAG (black), MAG_{2p} (blue), and $MAGA_{2p}$ (red). Bars indicate stimulation pulses applied to open (one-photon pulses in violet and blue, two-photon pulses in gray) and close LiGluR (one-photon pulses in green). Irradiation wavelengths are given in each case. Two-photon excitation conditions: MAG (λ = 820 nm, 10 scans of 0.4 s, 38 mW on sample), MAG_{2p} (λ = 900 nm, 0.4 s scan, 30 mW on sample), and $MAGA_{2p}$ (λ = 880 nm, 0.4 s scan, 42 mW on sample).

for a similar compound[21] (Figure 4d and Table S1 in the Supporting Information). An additional peak is observed for $MAGA_{2p}$ at λ = 360 nm, which lies very close to the absorbance band of the naphthalene moiety (see Figure 2a). Thus, sensitization of the azobenzene photoisomerization by the antenna also occurs when the photoswitch is conjugated to LiGluR. In addition, the time course of the MAG_{2p} and $MAGA_{2p}$ one-photon currents (blue and red traces in Figure 5a) confirms that fast spontaneous *cis*–*trans* back-isomerization and channel closure takes place after the illumination is switched off, while it requires irradiation with green light for MAG (black trace in Figure 5a). By fitting the one-photon current decays in the dark with monoexponential functions, the lifetimes of *cis*-MAG_{2p} and *cis*-$MAGA_{2p}$ tethered to LiGluR were determined to be 150 and 265 ms, respectively (Table S1 in the Supporting Information). These values are larger than those measured in solution (see above), which suggests that the ligand-binding site interaction slows down the thermal *cis*–*trans* isomerization of the azobenzene-based switches. This effect is enhanced for $MAGA_{2p}$ probably due to additional hydrophobic interactions and/or steric hindrance effects arising from the tethered naphthalene antenna.

Using a custom-built multiphoton setup where a tightly focused fs laser is raster scanned over the cells of interest, all three PTLs display robust and LiGluR-specific photocurrents in living cells that first demonstrate two-photon stimulation with NIR light of a synthetic photoswitchable protein (Figure 5b and Figures S9 and S10 in the Supporting Information). The amplitude of the responses follows the characteristic power dependence of two-photon absorption processes (Figure S11 in the Supporting Information) and corresponds to 10–20% of the photocurrent under one-photon excitation (Table S2 in the Supporting Information). In order to optimize the multiphoton

dx.doi.org/10.1021/ja5026326 | J. Am. Chem. Soc. 2014, 136, 8693–8701

stimulation conditions we characterized the two-photon action spectrum of each PTL (Figure 6a). The wavelength that yields maximal two-photon responses of MAG is around 820 nm. Repeated cell raster scans are required to get a saturating photocurrent from all available receptors (black trace in Figure 5b). Then, the current remains stable without laser illumination until LiGluR is closed with 500 nm light via one-photon *cis*–*trans* back-photoisomerization. The MAG_{2p} two-photon action spectrum is red-shifted and yields maximum current amplitude around 900 nm. The reduced currents obtained from $MAGA_{2p}$ hindered the acquisition of a detailed action spectrum, but are sufficient to identify two spectral ranges allowing two-photon activation of LiGluR: the first can be found at ~880 nm (corresponding to the direct absorbance of azobenzene, as in MAG_{2p}), and the second is located around 740 nm and is consistent with the naphthalene-sensitized photoisomerization.[34]

Remarkably, multiphoton currents mediated by MAG_{2p} and $MAGA_{2p}$ completely saturate after a few laser scans of the recorded cell (blue and red traces in Figure 5b). In addition, their rapid relaxation allows LiGluR to close immediately after the end of each stimulus, with time constants similar to those obtained with one-photon illumination (Table S2 in the Supporting Information), which enable fast, repeated activation of the receptor without requiring a second irradiation source for deactivation. Thus, the novel compounds MAG_{2p} and $MAGA_{2p}$ enable single-wavelength, multiphoton gating of LiGluR. However, MAG achieves higher two-photon current amplitudes than MAG_{2p} and $MAGA_{2p}$ in the long term (Figure 6b), because the thermal stability of its *cis* isomer allows building up a larger population of open-state channels upon repeated cell raster scans (Figure S12 in the Supporting Information). To compare the efficacy of LiGluR activation between PTLs, we calculated the ratio between two-photon and one-photon maximal responses (Figure 6c). Noticeably, MAG_{2p} and $MAGA_{2p}$ (both via direct and sensitized azobenzene excitation) display a higher ratio than MAG, thereby demonstrating that the efficiency of multiphoton isomerization was enhanced by the design of the new photoswitches.

After characterizing the two-photon stimulation of LiGluR, we pursued physiological applications that exploited the ability of this receptor to rapidly activate neurons[37] and trigger calcium-regulated processes.[38,39] The stimulation of individual neurons in micrometric volumes and millisecond time scales has been demonstrated using two-photon neurotransmitter uncaging[23] and optogenetics.[24,25] To complement this set of tools for investigating brain connectivity, we applied two-photon activation of LiGluR in neuronal and non-neuronal cells of the brain using the high photocurrents provided by MAG and MAG_{2p}. We expressed GluK2-L439C-eGFP in cultured hippocampal neurons, incubated them in MAG_{2p} and recorded neuronal activity using whole-cell patch clamp (Figures 7). Excitation of the soma with 900 nm light elicits inward currents in voltage-clamp experiments (Figure 7c). In current-clamp mode, these photocurrents triggered action potentials in two

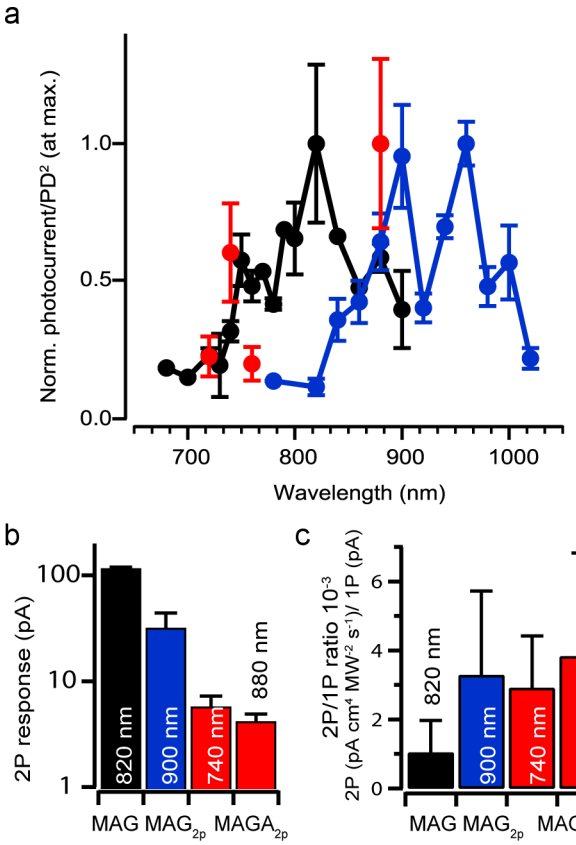

Figure 6. (a) Two-photon action spectra of LiGluR-MAG (black) and LiGluR-MAG_{2p} (blue) and two-photon activation of LiGluR-$MAGA_{2p}$ (red) at selected wavelengths. Photocurrent amplitudes were corrected for the different power densities used (PD), averaged over all cells measured, and normalized to the spectral maximum. (b) Absolute two-photon (2P) responses at the optimal wavelength. For $MAGA_{2p}$ values are given for sensitized (λ = 740 nm) and direct (λ = 880 nm) azobenzene excitation. (c) Ratio between the two- and one-photon responses (2*P*/1P). To compare between different LiGluR-tethers, two-photon responses were corrected for the distinct power densities and excitation times used and averaged over all cells measured. In all spectra here, N = 1–6 cells and errors are SEM.

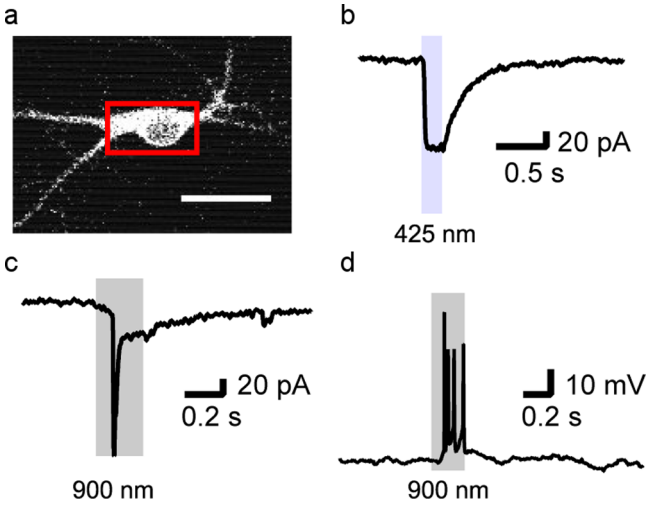

Figure 7. (a) Two-photon image (λ = 1000 nm) of a cultured LiGluR-MAG_{2p} hippocampal neuron filled with Alexa Fluor 594. Red square defines the raster scan area of two-photon stimulation. Scale bar is 20 μm. (b) Voltage-clamp recording during one-photon stimulation (blue bar). (c,d) Two-photon raster scan (gray bars) of the same neuron during (c) voltage-clamp recording, which shows two-photon current with a transient current spike (two-photon mean current amplitude: 21 ± 3 pA, 19 ± 2% of one-photon current, N = 3), and (d) current-clamp recording (resting potential = −45 mV). Two-photon excitation conditions: λ = 900 nm, 0.25 s scan, and 24 mW on sample.

dx.doi.org/10.1021/ja5026326 | J. Am. Chem. Soc. 2014, 136, 8693–8701

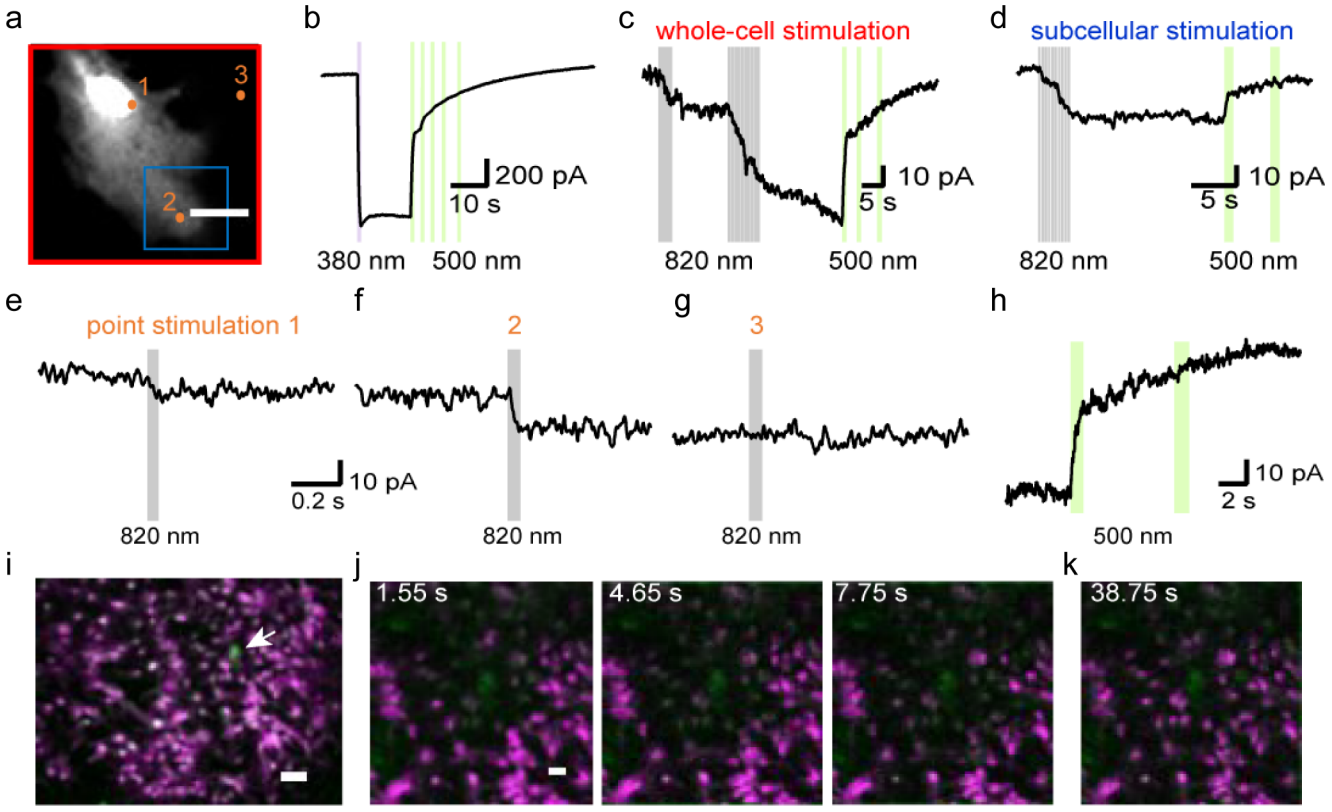

Figure 8. (a) Two-photon image (λ = 1000 nm) of a cultured LiGluR-MAG astrocyte filled with Alexa Fluor 594. Red and blue squares define the whole cell and subcellular raster scan areas, respectively. Locations of point stimulations are depicted by orange dots. Scale bar is 10 μm. (b) Whole-cell voltage-clamp recording of the astrocyte during one-photon stimulation (LiGluR opening, purple bar; LiGluR closing, green bar). (c–h) Two-photon currents measured on the same astrocyte (LiGluR opening, gray bar; one-photon LiGluR closing, green bar): (c) cell scan stimulation at λ = 820 nm, 10 scans of 0.7 s and 37 mW on sample (mean current amplitude: 60 ± 20 pA, 30 ± 10% of one-photon current, N = 2); (d) subcellular scan stimulation at λ = 820 nm, 10 scans of 0.25 s and of 68 mW on sample (mean current amplitude: 17 ± 9 pA, N = 2); (e–g) single-point stimulation (gray bar) at λ = 820 nm, 50 ms and 68 mW on sample (points 1 and 2 are on the cytoplasm, and point 3 is out of the cell as control); (h) LiGluR closing at the end of the stimulation protocol (green bar). (i–k) Two-photon calcium imaging of cultured astrocytes loaded with Fura-2 (in purple, λ = 800 nm) overlapped with an image of GFP fluorescence (in green, λ = 900 nm) to identify astrocytes expressing LiGluR-MAG. Scale bar is 20 μm, except 50 μm in (i). (j) Images at 1.55, 4.65, and 7.75 s after targeting the astrocyte to which the arrow points in (i) with two-photon stimulation (20 targets, 16-pixel diameter, 10 ms per point at λ = 800 nm, 60 mW on sample). (k) Recovery of intracellular calcium levels 38.75 s after stimulation.

out of three tested neurons (Figure 7d). Although several properties of LiGluR-MAG$_{2p}$ must be improved in order to reliably photocontrol whole neurons and individual presynaptic terminals (lifetime of the *cis* isomer, receptor expression level, and subcellular localization), these results indicate that it is possible to activate neurons using two-photon stimulation of synthetic photoswitchable proteins.

In the same experimental conditions, no spikes were elicited by two-photon stimulation of LiGluR-MAG, probably due to the slow photoresponses shown in Figure 5b. However, the large, step-function photocurrents provided by MAG and the calcium permeability of GluK2[40] make LiGluR-MAG more attractive to trigger calcium-regulated processes[39,41] including astrocyte activation[38] (see also Figure S7 in the Supporting Information). In cultured astrocytes expressing LiGluR-MAG (Figures 8), two-photon excitation at 820 nm triggered bistable currents (Figure 8c). Interestingly, whole-cell photocurrents can also be measured during the stimulation of a subcellular region (Figure 8d) or a spot (Figures 8e–g), and these responses are reversible by illuminating the cell at 500 nm (Figures 8c,d,h). In order to verify whether such stimuli were enough to activate an intracellular calcium response in the astrocyte,[38,42] we performed two-photon calcium imaging together with two-photon stimulation of astrocytes expressing LiGluR-MAG. When we stimulated an expressing astrocyte, LiGluR activation caused a calcium increase that propagated to neighboring cells, generating a calcium wave that expanded to astrocytes throughout the field of view (Figure 8i–k and Movie S1 in the Supporting Information). This effect, which is not observed when locally stimulating non-expressing astrocytes (Figure S13 and Movie S2 in the Supporting Information), demonstrates that two-photon LiGluR activation can be used to manipulate cytosolic calcium levels in cultured astrocytes.

■ CONCLUSIONS

We have demonstrated the two-photon activation of azobenzene-based photoswitches in living cells expressing the light-gated receptor LiGluR.[26] Although a symmetrically substituted azobenzene was reported to photoisomerize under continuous-wave NIR excitation,[43] in general these chromophores present low two-photon absorption cross sections.[29,30] However, synthetic PTLs like MAG[26] offer great flexibility to adjust their photochemical properties without altering protein function. We have rationally designed MAG derivatives with visible absorption, fast thermal relaxation, and high two-photon isomerization efficacy based on push–pull substitu-

dx.doi.org/10.1021/ja5026326 | J. Am. Chem. Soc. 2014, 136, 8693–8701

tions[31,32,44,45] and sensitization[33] of the azobenzene photoisomerization. These modifications and the reported multiphoton excitation conditions should be directly applicable to all azobenzene-based bioactive ligands,[11] including intracellular photoswitches known to penetrate into cells directly[46] or through specific ion channels,[47] and hyperpolarizing step-function photoswitchable channels like SPARK[48] or LiGABA.[11] Our findings thus enable the use of synthetic photoswitches to manipulate extra- and intracellular biochemical processes with the spatiotemporal precision provided by two-photon stimulation.

EXPERIMENTAL SECTION

Synthesis. A detailed description of the synthesis of target photoswitchable tethered ligands is given in the Supporting Information.

Photochemical Characterization. *Trans*−*cis* isomerization of MAG_{2p} and $MAGA_{2p}$ in solution was investigated by (i) ^{1}H NMR for the elucidation of the photostationary-state mixtures; (ii) steady-state UV−vis absorption spectroscopy for *trans*−*cis* photoisomerization and slow *cis*−*trans* thermal back-isomerization processes; and (iii) transient absorption spectroscopy for fast *cis*−*trans* thermal back-isomerization processes.

LiGluR on Cultured Cells. HEK293 tsA201 cell line, cultured hippocampal neurons, and astrocytes plated on glass coverslips were transfected with GluK2-L439C-eGFP. Prior to each experiment, they were incubated with one of the PTLs to allow the chemical conjugation with the receptor channel and light sensitization. A second incubation with concavalin A was done in order to inhibit desensitization of the glutamate receptor.

Electrophysiology. For two-photon stimulation, voltage-clamp and current-clamp recordings under whole-cell configuration were done with an Axon Multiclamp 700B amplifier (Molecular Devices), and data were acquired at 10 kHz. Borosilicate glass pipettes were pulled with a typical resistance of 4−6 MΩ for HEK293 tsA201 cells and neurons or 7−8 MΩ for astrocytes. Bath solution was composed of 140 mM NaCl, 1 mM MgCl, 2.5 mM KCl, 10 mM HEPES, 2.5 mM $CaCl_2$, and 10−20 mM glucose to fix osmolarity to 310 mOsm·kg^{-1}, pH 7.42 adjusted with NaOH. For HEK293 tsA201 cell line, pipet solution contained 120 mM cesium methanosulfonate, 10 mM TEA-Cl, 5 mM $MgCl_2$, 3 mM Na_2ATP, 1 mM Na_2GTP, 20 mM HEPES, and 0.5 mM EGTA, 290 mOsm·kg^{-1}, pH 7.2 adjusted with CsOH. For neurons and astrocytes it consisted of 130 mM potassium gluconate, 5 mM NaCl, 10 mM HEPES, 0.1 mM EGTA, 2 mM $MgSO_4$, 4 mM Mg-ATP, 0.4 mM NaXGTP, 7 mM Na_2-phosphocreatine, 2 mM pyruvic acid, and 0.1 mM Alexa Fluor 594 (Molecular Probes), pH 7.3 adjusted with KOH.

Two-Photon Stimulation. All two-photon experiments were performed in the Yuste laboratory with a custom-made two-photon laser scanning microscope based on a modified Olympus BX50WI microscope with a Ti:sapphire laser as light source (Coherent Chameleon Ultra II, 140 fs pulses, 80-MHz repetition rate). Laser power was modulated by a Pockels cell (Conoptics) and adjusted for each wavelength to be close to 40 mW on sample for MAG_{2p} and $MAGA_{2p}$ and 50 mW on sample for MAG, if not specified otherwise. In experiments with MAG, we used a 20*x*/0.5-NA objective (Olympus), and with the red-shifted compounds, we used a 20*x*/0.95-NA objective (Olympus) in Figures 5 and 6 and a 40*x*/0.8-NA objective (Olympus) in Figures 7 and 8. For two-photon stimulation we defined a ROI and applied a unidirectional raster scan using FluoView software, or we performed point stimulations with custom-written LabView Software.[49]

Calcium Imaging of Astrocytes. First, 50 μL of DMSO was added to a 50 μg aliquot of Fura-2-AM (Life Technologies). Next, 0.2 μL of this solution and 0.2 μL of pluronic acid (20% in DMSO) in 2 mL supplemental media were added to the culture dish and incubated at 37 °C for 30 min, before washing and LiGluR conjugation with MAG and concanavalin A treatment. We raster-scanned Fura-2 (100 frames, 1.55 s/frame) at 800 nm and 40 mW on sample with a 20*x*/0.5-NA objective for recording the activity of astrocytes and stimulated single nonexpressing or GFP-positive astrocytes using custom written software,[49] with a protocol of 20 stimulation targets on the cell with a16-pixel diameter, corresponding to approximately 11 μm diameter.

Data Analysis. Amplitudes of LiGluR currents were analyzed using IgorPro (Wavemetrics), and closing time constants of LiGluR were determined with a custom-made software using LabView. In the two-photon action spectrum of each compound, every set of data from one cell was normalized to the action spectrum integral from a chosen representative before cell average. Finally, we normalized each action spectrum to its maximum. Calcium imaging of astrocytes was analyzed using custom written software (Caltracer) and ImageJ.

ASSOCIATED CONTENT

Supporting Information

General materials and methods, detailed description of the synthesis of MAG_{2p} and $MAGA_{2p}$, and additional photochemical (Figures S1−S6) and biological (Figures S7−S13, Tables S1 and S2, and Movies S1 <ja5026326_si_003.avi> and S2 <ja5026326_si_004.avi>) measurements. This material is available free of charge via the Internet at http://pubs.acs.org.

AUTHOR INFORMATION

Corresponding Authors

rmy5@columbia.edu
jordi.hernando@uab.cat
pau@icrea.cat

Author Contributions

[+]M.I.-S. and M.G.-M. contributed equally.

Notes

The authors declare no competing financial interest.

ACKNOWLEDGMENTS

We thank Dirk Trauner for providing us the MAG compound; Ehud Isacoff for supplying us with the GluK2-L439C-eGFP construct; Ariadna Pérez-Jiménez and Núria Camarero for subcloning it into pcDNA3; Yeonsook Shin, Alexa Semonche, and Masayuki Sakamoto for preparation of primary cultures and cell transfection; and Sònia Parés for synthesis at initial stages of the project. We are grateful to Darcy S. Peterka and Artur Llobet for helpful discussions. We acknowledge financial support from the RecerCaixa foundation (2010ACUP00378), the "Marató de TV3" foundation (111531), the Human Frontier Science Program (CDA022/2006), the European Research Council (ERC-2007-StG-210355 and ERC-2012-PoC-335011), the European Commission (FP7-ICT-2009-270483), the Catalan government (grant 2009-SGR-277 and fellowship 2012-FI_B 01122), the Universitat Autònoma de Barcelona (predoctoral fellowship of M.G.-M.), and the Spanish government (grants CTQ2008-06160, CTQ2012-30853, and CTQ2010-15380 and FPU fellowship AP2008-03313). The Yuste laboratory is supported by NIDA (R21DA034195), NIHM (R01MH101218) and Deutsche Forschungsgemeinschaft (Research fellowship HI 1728/1-1). This material is based upon work supported by the U.S. Army Research Laboratory and the U.S. Army Research Office under contract no. W911NF-12-1-0594 (MURI). This article is dedicated to Prof. Josep Font Cierco on the occasion of his 75th birthday.

REFERENCES

(1) Harvey, J. H.; Trauner, D. *ChemBioChem* **2008**, *9*, 191.

(2) Yamada, M. D.; Nakajima, Y.; Maeda, H.; Maruta, S. *J. Biochem.* **2007**, *142*, 691.
(3) Wu, Y. I.; Frey, D.; Lungu, O. I.; Jaehrig, A.; Schlichting, I.; Kuhlman, B.; Hahn, K. M. *Nature* **2009**, *461*, 104.
(4) Umeki, N.; Yoshizawa, T.; Sugimoto, Y.; Mitsui, T.; Wakabayashi, K.; Maruta, S. *J. Biochem.* **2004**, *136*, 839.
(5) Schierling, B.; Noël, A. J.; Wende, W.; Hien, l. T.; Volkov, E.; Kubareva, E.; Oretskaya, T.; Kokkinidis, M.; Römpp, A.; Spengler, B.; Pingoud, A. *Proc. Natl. Acad. Sci. U.S.A.* **2010**, *107*, 1361.
(6) Asanuma, H.; Liang, X.; Nishioka, H.; Matsunaga, D.; Liu, M.; Komiyama, M. *Nat. Protoc.* **2007**, *2*, 203.
(7) Ito, H.; Liang, X.; Nishioka, H.; Asanuma, H. *Org. Biomol. Chem.* **2010**, *8*, 5519.
(8) Airan, R. D.; Thompson, K. R.; Fenno, L. E.; Bernstein, H.; Deisseroth, K. *Nature* **2009**, *458*, 1025.
(9) Oh, E.; Maejima, T.; Liu, C.; Deneris, E.; Herlitze, S. *J. Biol. Chem.* **2010**, *285*, 30825.
(10) Miesenbock, G. *Science* **2009**, *326*, 395.
(11) Kramer, R. H.; Mourot, A.; Adesnik, H. *Nat. Neurosci.* **2013**, *16*, 816.
(12) Toettcher, J. E.; Gong, D.; Lim, W. A.; Weiner, O. D. *Nat. Methods* **2011**, *8*, 837.
(13) Denk, W.; Strickler, J. H.; Webb, W. W. *Science* **1990**, *248*, 73.
(14) Papagiakoumou, E.; Begue, A.; Leshem, B.; Schwartz, O.; Stell, B. M.; Bradley, J.; Oron, D.; Emiliani, V. *Nat. Photonics* **2013**, *7*, 274.
(15) Oron, D.; Papagiakoumou, E.; Anselmi, F.; Emiliani, V. *Prog. Brain Res.* **2012**, *196*, 119.
(16) Watson, B. O.; Nikolenko, V.; Yuste, R. *Front. Neural Circuits* **2009**, *3*, 6.
(17) Yizhar, O.; Fenno, L. E.; Prigge, M.; Schneider, F.; Davidson, T. J.; O'Shea, D. J.; Sohal, V. S.; Goshen, I.; Finkelstein, J.; Paz, J. T.; Stehfest, K.; Fudim, R.; Ramakrishnan, C.; Huguenard, J. R.; Hegemann, P.; Deisseroth, K. *Nature* **2011**, *477*, 171.
(18) Wen, L.; Wang, H.; Tanimoto, S.; Egawa, R.; Matsuzaka, Y.; Mushiake, H.; Ishizuka, T.; Yawo, H. *PLoS One* **2010**, *5*, e12893.
(19) Gorostiza, P.; Isacoff, E. Y. *Physiology* **2008**, *23*, 238.
(20) Mourot, A.; Kienzler, M. A.; Banghart, M. R.; Fehrentz, T.; Huber, F. M.; Stein, M.; Kramer, R. H.; Trauner, D. *ACS Chem. Neurosci.* **2011**, *2*, 536.
(21) Kienzler, M. A.; Reiner, A.; Trautman, E.; Yoo, S.; Trauner, D.; Isacoff, E. Y. *J. Am. Chem. Soc.* **2013**, *135*, 17683.
(22) Fehrentz, T.; Kuttruff, C. A.; Huber, F. M.; Kienzler, M. A.; Mayer, P.; Trauner, D. *ChemBioChem* **2012**, *13*, 1746.
(23) Judkewitz, B.; Roth, A.; Häusser, M. *Neuron* **2006**, *50*, 180.
(24) Packer, A. M.; Peterka, D. S.; Hirtz, J. J.; Prakash, R.; Deisseroth, K.; Yuste, R. *Nat. Methods* **2012**, *9*, 1202.
(25) Prakash, R.; Yizhar, O.; Grewe, B.; Ramakrishnan, C.; Wang, N.; Goshen, I.; Packer, A. M.; Peterka, D. S.; Yuste, R.; Schnitzer, M. J.; Deisseroth, K. *Nat. Methods* **2012**, *9*, 1171.
(26) Volgraf, M.; Gorostiza, P.; Numano, R.; Kramer, R. H.; Isacoff, E. Y.; Trauner, D. *Nat. Chem. Biol.* **2006**, *2*, 47.
(27) Gorostiza, P.; Volgraf, M.; Numano, R.; Szobota, S.; Trauner, D.; Isacoff, E. Y. *Proc. Natl. Acad. Sci. U.S.A.* **2007**, *104*, 10865.
(28) Szymanski, W.; Beierle, J. M.; Kistemaker, H. A. V.; Velema, W. A.; Feringa, B. L. *Chem. Rev.* **2013**, *113*, 6114.
(29) De Boni, L.; Rodrigues, J. J.; dos Santos, D. S.; Silva, C.; Balogh, D. T.; Oliveira, O. N.; Zilio, S. C.; Misoguti, L.; Mendonça, C. R. *Chem. Phys. Lett.* **2003**, *374*, 684.
(30) De Boni, L.; Misoguti, L.; Zilio, S. C.; Mendonça, C. R. *ChemPhysChem* **2005**, *6*, 1121.
(31) Antonov, L.; Kamada, K.; Ohta, K.; Kamounah, F. S. *Phys. Chem. Chem. Phys.* **2003**, *5*, 1193.
(32) Magennis, S. W.; Mackay, F. S.; Jones, A. C.; Tait, K. M.; Sadler, P. J. *Chem. Mater.* **2005**, *17*, 2059.
(33) Jiang, D. L.; Aida, T. *Nature* **1997**, *388*, 454.
(34) Kim, H. M.; Cho, B. R. *Acc. Chem. Res.* **2009**, *42*, 863.
(35) Bandara, H. M. D.; Burdette, S. C. *Chem. Soc. Rev.* **2012**, *41*, 1809.
(36) Schanze, K. S.; Mattox, T. F.; Whitten, D. G. *J. Org. Chem.* **1983**, *48*, 2808.
(37) Szobota, S.; Gorostiza, P.; Del Bene, F.; Wyart, C.; Fortin, D. L.; Kolstad, K. D.; Tulyathan, O.; Volgraf, M.; Numano, R.; Aaron, H. L.; Scott, E. K.; Kramer, R. H.; Flannery, J.; Baier, H.; Trauner, D.; Isacoff, E. Y. *Neuron* **2007**, *54*, 535.
(38) Li, D.; Herault, K.; Isacoff, E. Y.; Oheim, M.; Ropert, N. *J. Physiol.* **2012**, *590*, 855.
(39) Izquierdo-Serra, M.; Trauner, D.; Llobet, A.; Gorostiza, P. *Biophys. J.* **2013**, *104*, 497A.
(40) Egebjerg, J.; Heinemann, S. F. *Proc. Natl. Acad. Sci. U.S.A.* **1993**, *90*, 755.
(41) Izquierdo-Serra, M.; Trauner, D.; Llobet, A.; Gorostiza, P. *Biochim. Biophys. Acta* **2013**, *1830*, 2853.
(42) Cornell-Bell, A. H.; Finkbeiner, S. M.; Cooper, M. S.; Smith, S. J. *Science* **1990**, *247*, 470.
(43) Zhang, Y.; Erdmann, F.; Fischer, G. *Nat. Chem. Biol.* **2009**, *5*, 724.
(44) Venkataramani, S.; Jana, U.; Dommaschk, M.; Sonnichsen, F. D.; Tuczek, F.; Herges, R. *Science* **2011**, *331*, 445.
(45) Sakamoto, R.; Kume, S.; Sugimoto, M.; Nishihara, H. *Chem.—Eur. J.* **2009**, *15*, 1429.
(46) Nevola, L.; Martín-Quirós, A.; Eckelt, K.; Camarero, N.; Tosi, S.; Llobet, A.; Giralt, E.; Gorostiza, P. *Angew. Chem., Int. Ed.* **2013**, *52*, 7704.
(47) Mourot, A.; Fehrentz, T.; Le Feuvre, Y.; Smith, C. M.; Herold, C.; Dalkara, D.; Nagy, F.; Trauner, D.; Kramer, R. H. *Nat. Methods* **2012**, *9*, 396.
(48) Banghart, M.; Borges, K.; Isacoff, E.; Trauner, D.; Kramer, R. H. *Nat. Neurosci.* **2004**, *7*, 1381.
(49) Nikolenko, V.; Poskanzer, K. E.; Yuste, R. *Nat. Methods* **2007**, *4*, 943.